Pathology - Research and Practice 215 (2019) 660–667

Contents lists available at ScienceDirect

Pathology - Research and Practice

journal homepage: www.elsevier.com/locate/prp

miR-23a-3p suppresses cell proliferation in oral squamous cell carcinomas by targeting FGF2 and correlates with a better prognosis

miR-23a-3p inhibits OSCC growth by targeting FGF2

Fubo Chen[a], Shengcai Qi[a], Xu Zhang[a], Jinjin Wu[a], Xi Yang[b,c,**], Raorao Wang[a,*]

[a] Department of Stomatology, Shanghai Tenth People's Hospital, Tongji University School of Medicine, Shanghai, 200072, China
[b] Department of Oral & MaxillofacialeHead & Neck Oncology, Ninth People's Hospital, Shanghai JiaoTong University School of Medicine, China
[c] Shanghai Key Laboratory of Stomatology & Shanghai Research Institute of Stomatology, National Clinical Research Center of Stomatology, China

ARTICLE INFO

Keywords:
OSCC
miR-23a-3p
FGF2
Prognosis

ABSTRACT

Oral squamous cell carcinomas (OSCCs) are one of the most ubiquitous malignancies the world over, and are accompanied by a high mortality. microRNAs (miRNAs) have increasingly garnered attention with regards to the roles they play in initiation and progression of various kinds of cancers, including OSCC. It has been reported, that miR-23a-3p promotes the development of tumors for prostate cancer, gastric cancer and gliomas. The functions of miR-23a-3p in OSCC however, remain unclear. In this study, fibroblast growth factor 2 (FGF2) is revealed as a direct target of miR-23a-3p, based on luciferase assays and immunoblotting. The expression of miR-23a-3p and FGF2 were found to be significantly downregulated and upregulated in OSCC tissues respectively. This indicates a reverse correlation between miR-23a-3p and FGF2 levels. Using *in vitro* approaches we ascertained that miR-23a-3p might contribute to the inhibition of growth and inhibition through increasing apoptosis in OSCC cells; while an inhibitor of miR-23a-3p could reverse this effect. Examination of a clinical cohort of OSCC patients suggested that reduced expression of miR-23a-3p is correlated with more advanced cancerous stage and poorer differentiation of OSCC cell. Additionally, a survival analysis and the Cox-hazard regression model showed that higher levels of miR-23a-3p can be used reliably for prognosis of OSCC patients. This study indicates that miR-23a-3p might suppress tumor proliferation, invasion and promote apoptosis of OSCC by targeting FGF2. miR-23a-3p has the potential to be used as prognostic indicator, and could be exploited as a therapeutic reagent for OSCC in the future.

1. Introduction

Oral squamous cell carcinoma (OSCC) is one of the most prevalent cancers affecting the head and neck region: The world has paid a price due to its low survival rate, < 50% of persons live longer than five years. According to global cancer statistics in 2012, OSCC is most common in South-Central Asia and Central and Eastern Europe [1]. To this day, consumption of alcohol and tobacco are considered to be the leading risk factors for the development of OSCC [2]. It is urgently required that we shed light on the genetic and molecular events within cells, which can reveal the underlying mechanisms for the initiation and development of OSCC. This would be paramount for creating potential therapeutic and/or interventional targets for OSCC.

MicroRNAs (miRNAs), which are some of the most studied small non-coding RNAs, have exhibited a versatile role in the development and progression of several cancers, including OSCC [3]. They primarily act by suppressing translation or promoting the degradation of the targeted messenger RNA (mRNA) [4,5], and thus, block the functions of the targeted genes. Previous studies have implied that, miRNAs either facilitates tumor progression or serves as a tumor suppressor in OSCC. Liu and colleagues showed that miR92b could contribute to tumor proliferation and the growth of OSCC both in vitro and in vivo by

---

Abbreviations: OSCC, oral squamous cell carcinoma; FGF2, fibroblast growth factor 2; AUC, Area Under Curve; 3′-UTR, 3′ untranslated region; OPMD, oral potentially malignant disorders; NC, negative control; OS, overall survival; PFS, progression-free survival; HR, hazard risk

[*] Corresponding author at: Department of Stomatology, Shanghai Tenth People's Hospital, Tongji University School of Medicine, 301 Middle Yanchang Road, Shanghai, 200072, China.

[**] Corresponding author at: Department of Oral & MaxillofacialeHead & Neck Oncology, Ninth People's Hospital, Shanghai JiaoTong University School of Medicine, 639 Zhizaoju Road, Shanghai, 200011, China.

E-mail addresses: yangxii16@163.com (X. Yang), raoraowang@hotmail.com (R. Wang).

https://doi.org/10.1016/j.prp.2018.12.021
Received 12 October 2018; Received in revised form 6 December 2018; Accepted 24 December 2018

binding to the NLK and activating the NF-κB pathway; suggesting the tumor potentiating role of miRNAs in OSCC [6]. Other studies however, have shown that miRNAs have a tumor inhibiting effect. After observing a dramatic downregulation of miR-338 in both OSCC tissues and cell lines, Liu et al reported that miR-338 might inhibit the growth and metastatic ability of OSCC cells by interacting with Neuropilin-1 (NRP1) [7]. By targeting GIT ArfGAP 1 (GIT1), miRNA-491-5p could potentially repress the invasion and metastasis of OSCC [8]. Therefore, studying miRNAs might provide an effective tool to modulate the development of OSCC. In a study regarding the molecular mechanisms of osthol-induced inhibition of metastasis of prostate cancer, Wen et al., identified miR-23a-3p as a primary downregulated miRNA in response to osthol treatment; in particular, miR-23a-3p could potentiate the invasive ability of prostate cancer cells by interacting with E-cadherin, decreasing its expression and enhancing cell motility [9]; miR-23a-3p has also been reported to play a role in the tumor progression of gastric cancer and gliomas [10,11]. Thus, the multifunctional role of miR-23a-3p in tumor development was of particular interest, to us especially its potential function in tumorigenesis of OSCC.

Fibroblast growth factor 2 (FGF2), also called basic fibroblast growth factor, is one of the FGF family members; which is expressed in many tissues and participates in a wide array of biological activities [12,13]. Recently, several studies have suggested that FGF2 plays a role in the malignant phenotype of OSCC, or in the malignant transformation from oral potentially malignant disorders (OPMD) [14–16]. For example, after tissue validation, an investigation by Li et al., suggested that there is a positive correlation between FGF2 and the tumor size of OSCC [15]. Another study assessed the efficacy of an anticancer agent and established an OSCC model. This model showed via immunochemistry and tumor growth arrest that there was a lower expression of FGF2; indicating the oncogenic role of FGF2 in OSCC progression [14]. Yang et al reported that miR-126 might function as a tumor suppressor of OSCC by targeting FGF2 [17], suggesting the regulatory potential of miRNA to control FGF2 expression.

Although the function of miR-23a-3p has been demonstrated in prostate cancer, its role in OSCC still remains unclear. Therfore, we hypothesized that miR-23a-3p might target FGF2 in OSCC in light of the possible effects of miRNA on FGF2, based on bioinformatics prediction. In this study, we confirmed a direct interaction between miR-23a-3p and FGF2. This study proposes that miR-23a-3p is capable of inhibiting tumor cell proliferation and improving the apoptotic proportion of OSCC cells, possibly by depressing the protein level of FGF2. Clinical tissue validation assays have implied that there is the potential to use miR-23a-3p in the prognosis of OSCC. This study has illuminated the mechanisms and functions of miR-23a-3p in the development of OSCC.

2. Materials and methods

2.1. Cell line and cell culture

Human oral squamous cell carcinoma cell lines and normal oral epithelial cell lines, including SCC9, SCC25, HSC4, CAL27, HEK, BEL, HOK and HOEC were purchased from the American Type Culture Collection (ATCC). Both types of cell lines were cultured in Dulbecco's Modified Eagle Medium (DMEM) supplemented with 10% fetal bovine serum (FBS) and 1% penicillin/streptomycin. The cells were maintained in a humid incubator with 5% CO2 at 37 °C. All media and reagents were purchased from Gibco; Thermo Fisher Scientific (USA).

2.2. OSCC specimens

One hundred and thirty-four paraffin-embedded OSCC samples and their cognate adjacent normal tissues were obtained from the Department of Oral & Maxillofaciale Head & Neck Oncology, Ninth People's Hospital, Shanghai JiaoTong University School of Medicine from 2002 to 2018. The clinical information was collected at the same time. A senior pathologist at the Ninth People's hospital applied a Hematoxylin and eosin-stain (HE) to the tissues to reassess the diagnosis. This study was approved by the Ethics Committee of the Ninth People's Hospital affiliated to Shanghai JiaoTong University School of Medicine and informed consent was acquired from all participants.

2.3. RNA extraction and qPCR

Total RNA was isolated from sections of the paraffin embedded OSCC samples and the adjacent normal tissues with the RNeasy FFPE Kit (Qiagen, USA) per the manufacturer's instructions. The total RNA of the OSCC cells and the normal oral epithelial cells were extracted with the QIAshredder and RNeasy Plus Mini Kit (Qiagen, USA) according to the manufacturer's instruction. RNA concentrations were determined by using a UV-2401 spectrophotometer (Shimadzu, Japan). For the preparation of cDNA, 1ug of total RNA was used as template in a reverse transcription reaction using PrimerScriptTM RT reagent kit (Takara, Japan). qPCR assays were utilized to quantitate the expression of individual genes; the reactions were conducted on a 7900 H T Real-Time PCR System (Applied Biosystems, USA) with the PowerUp SYBR Green Master Mix (Applied Biosystems, USA). The relative expression level of each gene was calculated by utilizing a 2-ΔΔct algorithm and normalized to GAPDH and U6, which served as internal controls for mRNA and miRNA, respectively. Primers for amplifying GAPDH, U6, miR-23a-3p, FGF2, and sequences of the miR-stem loop, miR-NC mimics, miR-NC inhibitor, miR-23a-mimics, and miR-23a-inhibitor were provided by Jima Biotech (Shanghai, China), the details were presented in Table 1.

Table 1
Primers for qPCR and sequences of miR-stem loop, miR-NC mimics, miR-NC inhibitor, miR-23a-mimics, and miR-23a-inhibitor.

Name	Sequence(5'-3')
GAPDH-F	GCACCGTCAAGGCTGAGAAC
GAPDH-R	TGGTGAAGACGCCAGTGGA
FGF2-F	TCAAGCAGAAGAGAGAGGAG
FGF2-R	CCGTAACACATTTAGAAGCC
miR-23a-3p RT1	GTTGGCTCTGGTGCAGGGTCCGAGGTATTCGCACCAGAGCCAACGGAAATCC
miR-23a-3p RT2	CGGCGGATCACATTGCCAGGG
stem loop	GTGCAGGGTCCGAGGT
U6F	CTCGCTTCGGCAGCACA
U6R	AACGATTCACGAATTTGCGT
NC mimics	ACUACUGAGUGACAGUAGA
NC inhibitor	CAGUACUUUUGUGUAGUACAA
miR-23a mimics	AUCACAUUGCCAGGGAUUUCC
miR-23a inhibitor	GGAAATCCCTGGCAATGTGAT

2.4. Reagents and cell transfection

The miR-23a-3p mimics, miR-23a-3p inhibitor and the controls including miR-NC and miR-NC inhibitor (iNC) were all chemically synthesized by Jima Biotech (Shanghai, China). Lipofectamine 2000 (Thermo Fisher Scientific, USA) was applied to the cell lines with the indicated reagents based on the manufacturer's protocol. HEK293 cell were co-transfected with 125 ng PGL3 vacant/ wtUTR-FGF/ mutUTR-FGF, 375 ng miR-NC/ miR-23a mimics/ miR-23a inhibitor (inh-23a)/ inhibitor NC (iNC) (Ambion, USA), as well as 10 ng pTK. HEK293 cell was detected at 24 h post transfection. The SCC25 and CAL27 cell lines were co-transfected with 2.5 μg miR-NC/ miR-23a mimics, and 75 pmol inh-23a/ iNC simultaneously. SCC25 and CAL27 cells were harvested before transfection and 24 h, 48 h, 72 h, 96 h post transfection.

2.5. Immunoblotting analysis

After transfection the cell lines were lysed with RIPA buffer supplemented with a protease inhibitor. The concentration of each protein was determined by a BCA assay with BCA kit (Thermo Fisher Scientific, USA). Next, equal amounts of protein for each sample were subjected to an SDS-PAGE gel electrophoresis and then transferred to polyvinylidene fluoride membranes. Subsequently, the membranes were blocked with 5% milk at room temperature for 1 h, after which they were incubated with the primary antibodies of FGF2 (1:1000, Abcam, USA) and GAPDH (1:200, Kangchen Bio-tech, China) at 4 °C overnight. GAPDH was used as the loading control. The membranes were then incubated with a HRP-conjugated secondary antibody and the bands from the immunoblott were visualized using an enhanced ECL system (Thermo Fisher Scientific, USA). The expression level of FGF2, relative to the amount of GAPDH was quantitated by Image J software.

2.6. Cell proliferation assay

Cell proliferation of the transfected cells was determined by the 3-(4, 5-dimethylthiazol-2-yl)-2,5-diphenyltetrazolium bromide (MTT) assay. Post transfection, 2000 cells in 100 ul of medium were seeded into each well of 96 well plates and cultured for four days. The proliferation level was analyzed every 24 h by adding MTT into each well and incubating for 4 h, after which the media was removed and 10 ul DMSO was supplemented to dissolve the MTT. The absorbances were measured at 490 nm by utilizing a microplate reader (Bio Rad, USA).

2.7. Transwell assay

24-well transwell chambers with an 8 μm pore polycarbonate membrane were utilized to detect the OSCC cells' invasion ability (Corning, USA). A matrigel matrix was used to pre-coat the membrane (BD, Franklin Lakes, USA). 4×10^5 suspended cells in serum-free medium were added to the upper chamber, and 500 μL of DMEM medium containing 10% FBS was added to the lower chamber. Cells were wiped off the upper chamber with cotton swabs after 24 h incubation periods, the cells in the lower chamber were fixed with 4% paraformaldehyde, stained with 0.1% crystal violet, and counted using a light microscope (Olympus, Japan).

2.8. Flow cytometric assay

A flow cytometric assay was conducted to measure the percentage of apoptotic cells under various treatments, using the AnnexinV-FITC/ PI Apoptosis Detection Kit (Abcam, USA). Specifically, at 48 h post transfection the cells were digested, washed twice in PBS and then a binding buffer was added. The cells were then stained with Annexin V-FITC and propidium iodide (PI). Lastly, the flow cytometric analysis was performed to determine the cell apoptosis rate with FlowJo V10 software.

2.9. Luciferase reporter assay

The luciferase reporter assay was conducted on the basis of manufacturer's instructions (Promega, USA). The 3′-UTR of FGF2, which putatively harbors the binding site of miR-23a-3p was amplified by PCR and cloned into the pGL3 vector between the HindIII and NheI sites. The pGL3-FGF2-mutant vector, created with 5 mismatches at the miR-23a-3p binding site of the 3′-UTR region, was generated as a negative control. Next, HEK293 T cells in 96-well plates were transfected with the pGL3-FGF2 or the pGL3-FGF2-mutant vector, along with miR-148a-3p. Additionally, control wells were transfected with just pGL3 and miR-NC. The luciferase activity was detected with the Dual-Luciferase Reporter Assay System (Promega, USA), and the relative luciferase activity was calculated by comparing the samples to the negative control.

2.10. HE staining

All the OSCC tissues that had a reduced or elevated expression levels of miR-23a-3p were selected for the histological analysis. The sections of the specimens were routinely stained with hematoxylin/eosin (HE). The differentiation level of all patient samples were evaluated by a senior pathologist, and the relationship between the expression levels of miR-23a-3p and the differentiation degree of OSCC were compared.

2.11. Statistical analysis

Statistical analyses were conducted with SPSS 20.0 (Chicago, USA) as well as GraphPad 6.0 (La Jolla, USA). The differences in the expression levels of miR-23a-3p and FGF2 between cancerous tissues and adjacent normal tissues were analyzed by a paired-samples t-test. The differences in the expression levels of miR-23a-3p and FGF2 between cancerous and normal epithelial cells were calculated by Student t-test. The relationship between the miR-23a-3p level and various clinicopathological parameters were assessed by Chi-square test. The correlation of miR-23a-3p and FGF2 was explored by Pearson correlation analysis. Univariate survival curves were plotted via the Kaplan–Meier method, and the differences of the overall survival rate and progression-free survival probability of patients with a low or high expression of miR-23a-3p were evaluated by log-rank test. A multivariate analysis for survival was performed by a Cox hazard regression model. A p value < 0.05 was considered statistically significant.

3. Results

3.1. miR-23a-3p is responsible for the reduced protein level of FGF2 in OSCC

We initially searched for the potential target genes of miR-23a-3p in OSCC by using publicly available databases including targetscan and miRbase. FGF2 was then suggested to be a putative target of miR-23a-3p. The binding site of miR-23a-3p is indicated to be in the 3′-UTR of FGF2 (Fig. 1A). In order to study the interaction between miR-23a-3p and FGF2, luciferase reporter vectors harboring 3′-UTR wt-FGF2 (wild type) or mut-FGF2 (mutant type) were constructed. Next, SCC25 cells were co-transfected with miR-NC and pGL3, miR-23a-3p and wt-FGF2, miR-23a-3p and mut-FGF2, respectively. As expected, miR-23a-3p suppressed the luciferase activity of the vector containing the wt-FGF2, but not that of the mut-FGF2 (Fig. 1B). Our results demonstrated that FGF2 is a direct target of miR-23a-3p in OSCC.

We then performed an *in vitro* assay by transfecting of OSCC cells. Our result indicated that the FGF2 expression levels were the most significantly reduced in the SCC25 and CAL27 among four OSCC cell lines (Fig. 1C). The addition of the miR-inhibitor could rescue the reduced effect and restore the level of FGF2 (Fig. 1D). The same result was obtained and confirmed via blotting of the CAL27 OSCC cell line

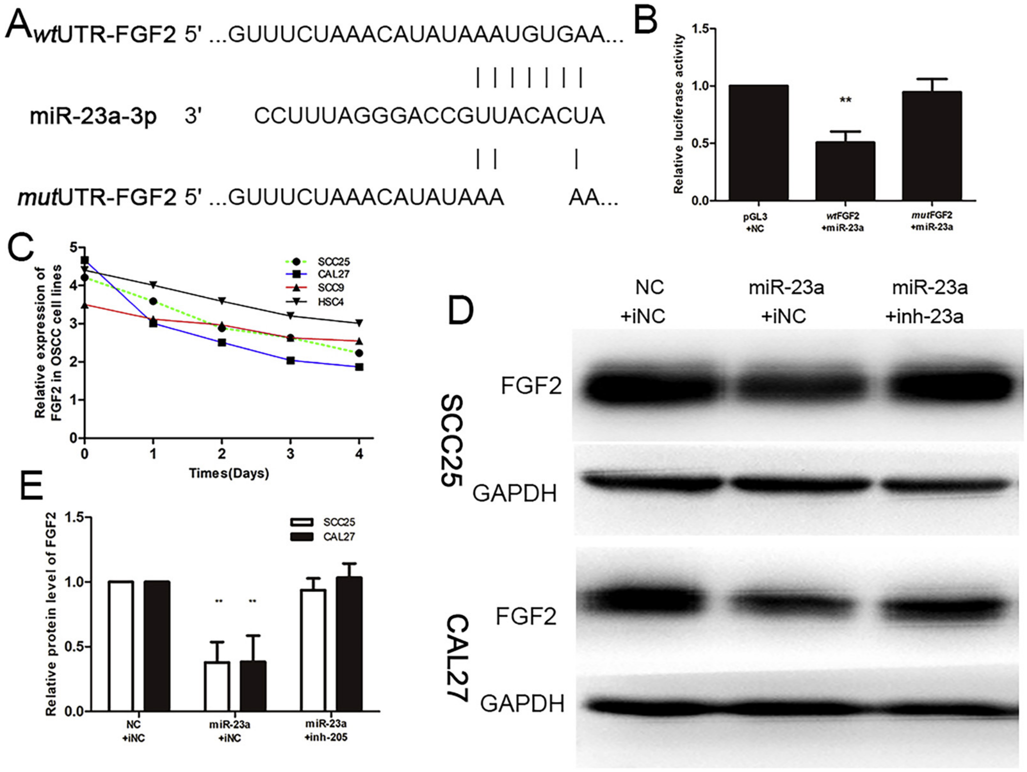

Fig. 1. FGF2 is a direct target of miR-23a-3p in OSCC.

A. miR-23a-3p directly targeted with FGF2 proved by luciferase reporter assay. B. miR-23a-3p has remarkably suppressed the luciferase activity of the vector containing wt-FGF2. C. FGF2 expression level reduced most significantly in cell lines SCC25 and CAL27 among four OSCC cell lines after transfected with miR-23a-3p mimics. D. Western blotting assay for detecting FGF2 expression in different co-transfected group of SCC25 and CAL27 cell line. E. Quantization of western result according to densitometry analysis in SCC25 and CAL27 cells, respectively. $*p < 0.05$, $**p < 0.01$ vs NC group.

(Fig. 1D). Additionally, image J software (1.51 w, National Institutes of Health, United States) was used to quantitate the level of FGF2 under various treatments in both the SCC25 and CAL27 OSCC cell lines. The results suggest a significant reduction of FGF2 levels under the overexpression of miR-23a-3p (Fig. 1E).

3.2. Inverse correlation between miR-23a-3p and FGF2 is presented in OSCC

The correlation between miR-23a-3p and FGF2 was further explored by using qPCR assays to measure the RNA levels of both in OSCC samples as well as their adjacent normal tissues and OSCC cell lines along with normal epithelial cells. The results revealed that the RNA level of miR-23a-3p was significantly lower in OSCC samples relative to the paired normal tissues (Fig. 2A). Similar differences were found in cancerous cell lines and normal epithelial cell lines (Fig. 2A). The expression level of FGF2 however was shown to be higher in OSCC tissues and cells when compared to the normal specimens and cells (Fig. 2B). Linear regression analysis revealed an inverse relationship between miR-23a-3p and FGF2 in both tissues and cells (Fig. 2C and D). Additionally, an AUC value of 0.778 validated the relatively high reliability of miR-23a-3p (Fig. 2E).

3.3. miR-23a-3p might inhibit the proliferation, invasion and promote the apoptosis of OSCC

We investigated the potential biological function of miR-23a-3p in OSCC by performing MTT and flow cytometric assays. First, we found that the relative proliferation rate of OSCC cells was significantly inhibited by an increased miR-23a-3p level. The co-transfection with miR-inhibitor reverses the suppressed proliferation of the SCC25 and CAL27 cells (Fig. 3A). Additionally, overexpression of miR-23a-3p in OSCC cells contributes to a marked increase of the Annexin-V positive cell population; which were ˜ 2-fold and 3-fold higher than the cells transfected with just miR-NC in the SCC25 and CAL27 cell lines, respectively. The addition of an miRNA inhibitor could reduce cell apoptosis (Fig. 3B and D). A Matrigel invasion assay was used to evaluate whether miR-23a-3p would affect the invasion of the SCC25 and CAL27 cell lines. The results demonstrated that overexpression of miR-23a-3p reduced the invasive ability of both of these cell lines (Fig. 3C and E). These results show that miR-23a-3p could contribute to the inhibition of cell proliferation and invasion of OSCC cells, and promote apoptosis.

3.4. Correlation between miR-23a-3p level and clinicopathological feature of OSCC

We attempted to address the significance of downregulated miR-23a-3p in OSCC patients by assessing the relationship between the expression of miR-23a-3p and the clinicopathological parameters of the 134 OSCC samples. Based on the Chi-square test, a lower level of miR-23a-3p was shown to be significantly correlated with a higher clinical stage and poor to moderate differentiation of OSCC: No other clinicopathological feature however, was found to be correlated with the expression of miR-23a-3p (Table 2). By conducting an H&E staining of OSCC tissues, the samples that exhibit higher levels of miR-23a-3p are most likely presents as well differentiation of tumor (Fig. 4C), while samples that exhibit low levels of miR-23a-3p are most likely presents as moderate and poor differentiation (Fig. 4A and B), which is in accordance with the findings of our clinicopathologic study.

3.5. Higher level of miR-23a-3p predicts better prognosis of OSCC patients

The overall survival (OS) and progression free survival (PFS) of OSCC patients were both evaluated with the Kaplan–Meier statistics. Our results indicate that the OS (p = 0.046) and progression free survival (p = 0.033) of patients with a higher expression of miR-23a-3p, were both significantly increased (Fig. 5A and B). We then included sex, age, location, tumor size, differentiation degree, TNM stage, lymph node status and serum level miR-23a-3p into the Cox-hazard regression model, and found that, the hazard risk (HR) for death (p = 0.002, HR = 2.059) and disease progression (p = 0.002, HR = 2.770) were

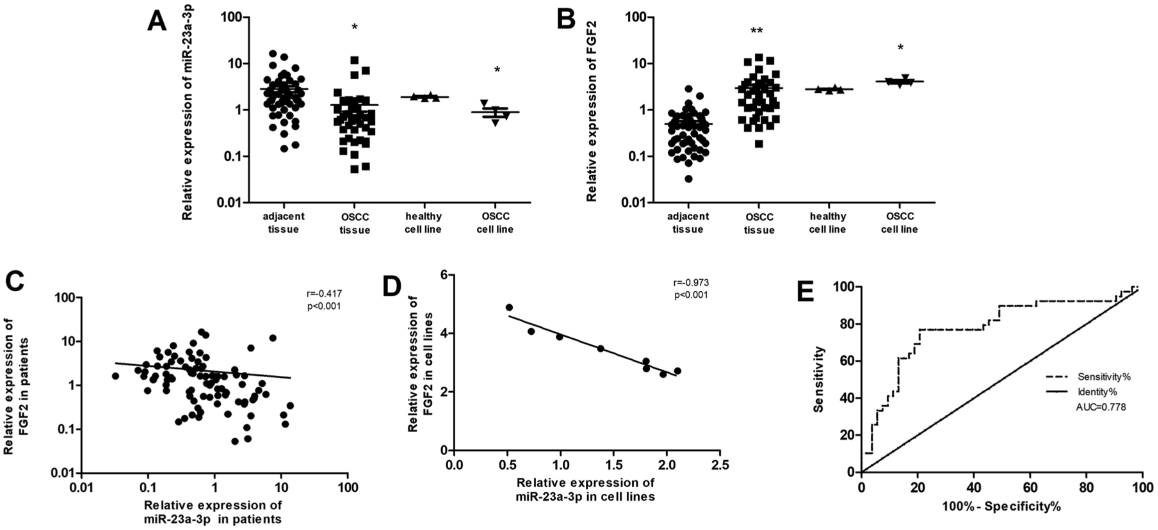

Fig. 2. Correlation between the relative expression levels of miR-23a-3p and FGF2 in OSCC.

A. Relative expression level of miR-23a-3p in adjacent normal tissue/cell lines and cancerous tissue/cell lines; B: Relative expression level of FGF2 in adjacent normal tissue and cancerous tissue as well as in normal or OSCC cells. C. The correlation between FGF2 and miR-23a-3p in patients' cohort with OSCC was performed by linear regression analysis. D. The correlation between FGF2 and miR-23a-3p in OSCC or oral normal epithelial cell lines was conducted by linear regression analysis. E. ROC curve for miR-23a-3p in patients' cohort with OSCC. $^{*}p < 0.05$, $^{**}p < 0.01$ vs NC group.

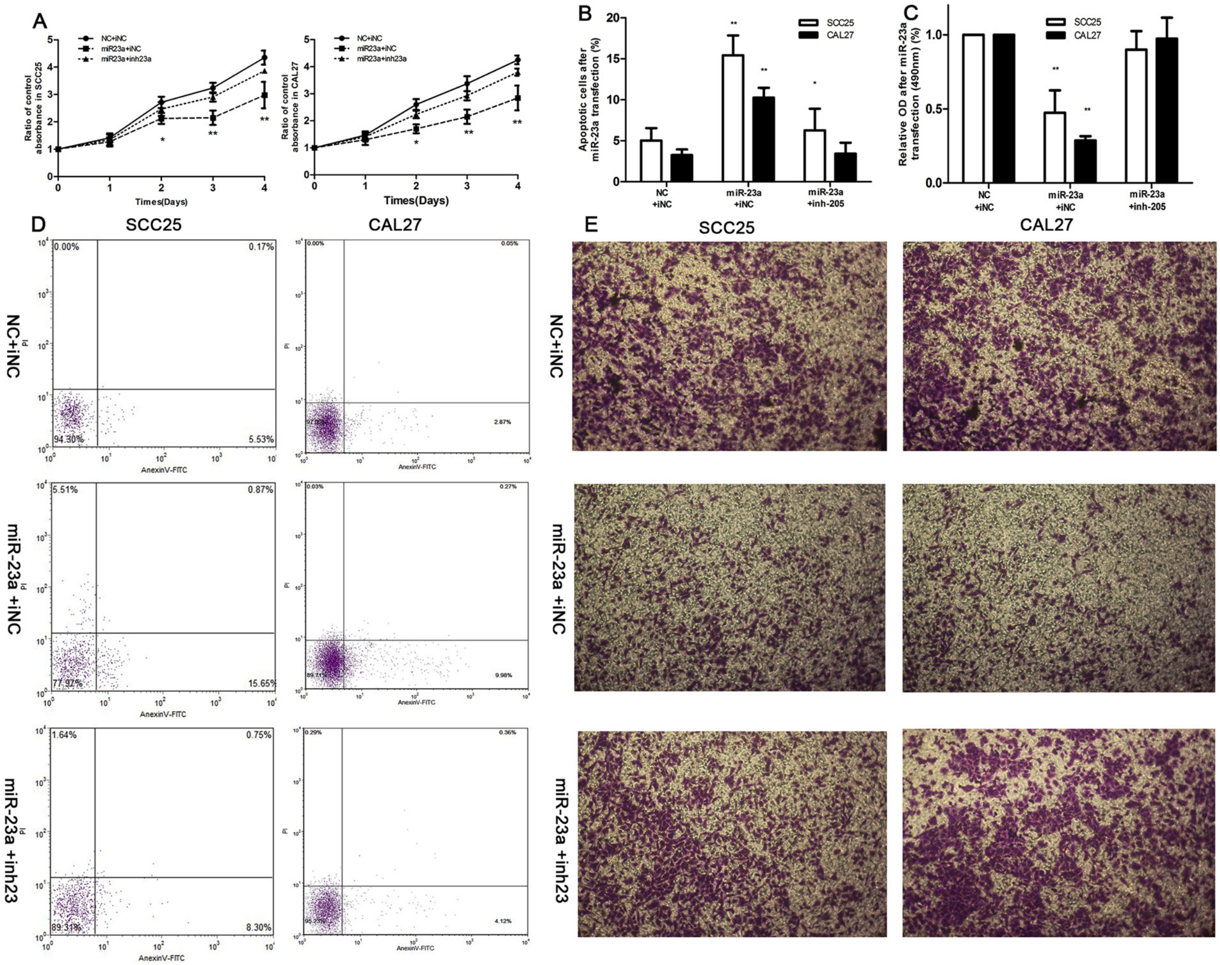

Fig. 3. Biologic effects of miR-23a-3p transfection in OSCC cell lines by MTT assay.

A. Grow curve of SCC25 proliferation after miR-23a-3p transfection. Co-transfection with miR-inhibitor could reverse the suppressed proliferation of SCC25 and CAL27 cells. B. Histograms of SCC25 and CAL27 cell lines apoptosis rates after miR-23a-3p transfection. C. Histograms of SCC25 and CAL27 invasion cells after miR-23a-3p transfection. D. Dot blot of Annexin V expression of SCC25 and CAL27 cells on 96 h after transfection. E. Invasive ability of SCC25 and CAL27 cells after miR-23a-3p transfection. $^{*}p < 0.05$, $^{**}p < 0.01$ vs NC group.

Table 2
Correlation of miR-23a-3p with clinical features of OSCC patients.

	cases (n = 134)	miR-23a-3p		χ^2	P value
		low (n = 67)	high (n = 67)		
Sex					
male	69 (51.49%)	32 (47.76%)	37 (55.22%)	0.311	0.577
female	65 (48.51%)	35 (52.24%)	30 (44.78%)		
Age (Y)					
≤60	70 (52.23%)	36 (53.73%)	34 (50.75%)	2.705	0.1
>60	64 (47.76%)	31 (46.27%)	33 (49.25%)		
Localization					
gingiva	28 (20.90%)	12 (17.91%)	16 (23.88%)	2.189	0.534
buccal mucosa	31 (23.13%)	17 (25.37%)	14 (20.90%)		
tongue	25 (42.54%)	31 (46.27%)	26 (38.81%)		
Other	18 (13.43%)	7 (10.45%)	11 (16.42%)		
Tumor size (cm)					
≤4	81 (60.45%)	43 (64.18%)	38 (56.72%)	0.78	0.377
>4	53 (39.55%)	24 (35.82%)	29 (43.28%)		
Clinical stage					
I/II	39 (29.10%)	14 (20.90%)	25 (37.31%)	4.376	0.036
III/IV	95 (70.90%)	53 (79.10%)	42 (62.69%)		
Differentiation					
Well	56 (41.79%)	22 (32.84%)	34 (50.75%)	4.418	0.036
Moderate/ Poor	78 (58.21%)	45 (67.16%)	33 (49.25%)		
Lymph node involvement					
No	54 (40.30%)	26 (38.81%)	28 (41.79%)	0.124	0.725
Yes	80 (59.70%)	41 (61.19%)	39 (58.21%)		

significantly increased in patients' group, with high level of miR-23a-3p (Table 3). This suggests that high miR-23a-3p expression might serve as an independent indicator for a better prognosis for OSCC patients.

4. Discussion

miRNAs, as one of the common categories of small non-coding RNAs, can post-transcriptionally control the gene expression by binding to the 3′-untranslated regions (UTR) mRNAs [9], It has been suggested that miRNAs deregulate in a variety of cancers and are reported to exert their effects on modulating the growth and metastasis of cancers [10,11]. miRNA-23a-3p has recently been shown to robustly function in the progression of several cancers. Wen et al., carried out a study which showed that there was a promoting effect of miRNA-23a-3p on prostate cancer metastasis, repressing the E-cadherin expression [9]. Additionally, after determining that there was a higher than normal expression of miRNA-23a-3p in gastric cancer tissues and cells, Li et al conducted an in vitro study which revealed sprouty homolog 2 (SPRY2) as a direct target of miRNA-23a-3p, wherein it mediates a promoting role of miRNA-23a-3p in tumor growth and metastasis of gastric cancer [10]. Hu and colleagues demonstrated that miRNA-23a-3p might contribute to the invasion of glioma cells by targeting homeobox D10 (HOXD10). [11] As the role of miRNA-23a-3p in OSCC remains uncharacterized, we decided to conduct this study. FGF2 has also been shown to be an important player in the initiation and development of OSCC. Wakulich et al revealed that there is increased expression of FGF2 associated with progression from epithelial dysplasia to OSCC [16]. Based on previous reports, miR-503 and miR-16 repress the tumor growth and proliferation of hepatocellular carcinomas and nasopharyngeal carcinomas respectively by targeting FGF2 [18,19]. Given the potent effect that miRNA-23a-3p has on other cancers and the possible interaction between miRNA and FGF2, we launched this study to uncover the role of miRNA-23a-3p in OSCC and explored the possible associations between miRNA-23a-3p and FGF2 in the progression of OSCC.

In this study, a luciferase assay was conducted to investigate whether FGF2 might serve as a direct target of miR-23a-3p in OSCC and the decreased luciferase activity validated our hypothesis. A qPCR assay was then performed to detect the expression level of miRNA-23a-3p and FGF2 in OSCC tissues along with their adjacent tissues for additional proof. As a result, the level of FGF2 and miRNA-23a-3p were indicated to be significantly higher and lower in OSCC samples respectively. The correlation analysis suggested a significant inverse relationship between miRNA-23a-3p and FGF2, and this explains the different expression levels of miRNA-23a-3p and FGF2 within the OSCC. By applying miRNA-23a-3p mimics in the presence or absence of its inhibitors into OSCC cells, a notable reduction of the protein level of FGF2 was observed under the induction of miRNA-23a-3p in both SCC25 and CAL27 cells. Thus, miR-23a-3p could target and downregulate the expression of FGF2 in OSCC cell lines. In previous studies,

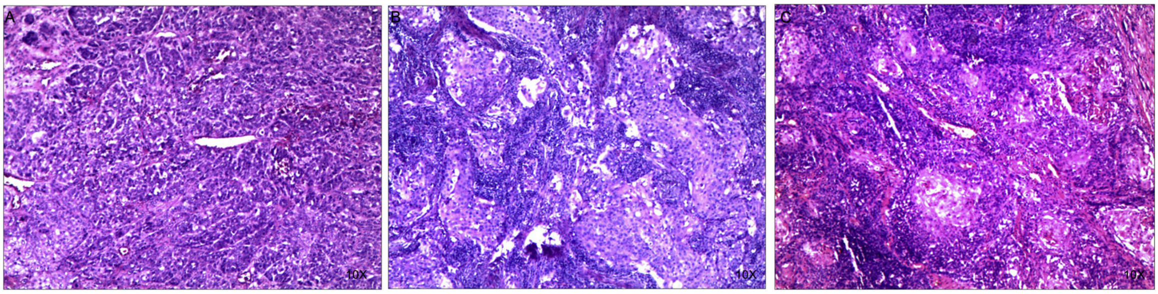

Fig. 4. Different degrees of differentiation in OSCC tissues.
A. H&E staining of poor differentiated OSCC tissues. B. H&E staining of moderate differentiated OSCC tissues. C. H&E staining of well differentiated OSCC tissues.

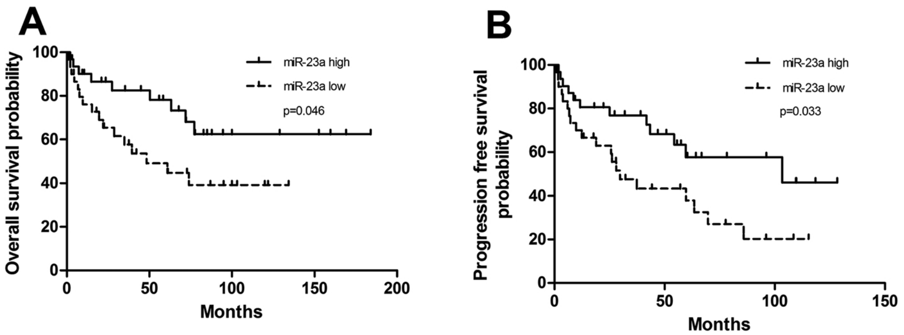

Fig. 5. Univariate Analysis of Survival for miR-23a-3p expression level in OSCC Patients.
A. Kaplan-Meier analysis for OS in patients with different level expression of miR-23a-3p. B. Kaplan-Meier analysis for PFS in patients with different expression level of miR-23a-3p.

Table 3
Multivariate Cox Proportional Hazard Analysis of Prognostic Factors for Survival of OSCC Patients.

Factors	Categories	OS		PFS	
		HR(95%CI)	P	HR(95%CI)	P
Sex	Male/ Female	0.748(0.405-1.741)	0.226	0.632(0.303-1.472)	0.291
Age	> 60/ ≤ 60	0.822(0.509-1.432)	0.305	0.728(0.440-1.335)	0.338
Localization	buccal mucosa/Others	0.816(0.523-1.318)	0.522	0.921(0.604-1.329)	0.626
Tumor size	> 4/ ≤ 4	1.419(0.319-4.568)	0.634	1.362(0.208-3.511)	0.509
TNM stage	III + IV/I + II	4.180(1.552-6.750)	< 0.001	3.524(1.029-5.887)	< 0.001
Differentiation	Moderate + High/Poor	0.821(0.440-1.809)	0.031	0.630(0.241-1.543)	0.027
Lymph node involvement	Yes/No	2.661(1.732-4.200)	0.024	2.569(1.377-3.601)	0.008
miR-23a-3p level	Low/High	2.059(1.064-3.227)	0.002	2.770(1.825-3.903)	0.013

HR: Hazard ratio; 95% CI: 95% Confidence interval; TNM: Tumor nodal metastases.

miR-23a-3p was reported to directly target various mRNAs such as ATG12 [20], CDH1 [21,22], FOXP2 [23], MT2A [24] and ESRP1 [25]; and thus regulate the biological behavior of melanoma, breast cancer, neuroblastoma and gastric cancer. In this study, we found a direct target of miR-23a-3p, which may provide a new avenue for treating OSCC.

FGF2 has previously been reported as an oncogene which facilitates the development of OSCC [14–16]. We performed in vitro assays to figure out the precise role of miR-23a-3p in OSCC. After overexpression of miR-23a-3p in SCC25 and CAL27 cells, the cell growth was inhibited and apoptosis was dramatically enhanced; while the miRNA inhibitor reversed the effect, which implies a potentially suppressive role for miR-23a-3p on OSCC progression. Other previous studies showed that miR-23a can exhibit proapoptotic functions [26], which supports our findings. In most prior studies, miR-23a was reported to be overexpressed in several tumors and promote invasion or metastasis [22–25,27]. There have, however, been a few reports that demonstrated that a down-regulated miR-23a could contribute to the progressive behavior of tumors [20,28]. In our study, when miR-23a-3p was overexpressed, the invasion ability of OSCC was inhibited. This suggests that the function of miR-23a in human tumors is complex.

The clinicopathological analysis shows an association between lower miR-23a-3p levels and a higher clinical stage as well as poor to moderate differentiation of OSCC. Though a larger tumor size is more frequently present in the higher level miR-23a-3p group (43.28% vs 35.82%), the tumor size was not found to statistically correlate with miR-23a-3p expression; which was inconsistent with our in vitro findings. This could possibly be attributed to the limited number of clinical samples. A higher level of miR-23a-3p appears to be prognostic of an improved OSCC outcome based on the survival analysis. This implies a possible application for miR-23a-3p as a robust prognosticator in future clinical settings.

Despite the reported function and findings of FGF2 as a downstream target of miR-23a-3p, the detailed functions and mechanisms of miR-23a-3p in OSCC are still insufficiently characterized. First, as miR-23a-3p is reported to be an oncogenic miRNA which promotes tumor progression such as in gastric cancer and glioma [10,11], which is the opposite finding of this study, including growth inhibition and increasing apoptosis, awaits to be validated in more OSCC cell lines other than SCC25 and CAL27. Second, a larger clinical cohort is required to better characterize the association between miR-23a-3p and tumor size, which we attempted to validate with our in vitro assays. Third, an in vivo study should be conducted to confirm the influence of miR-23a-3p on OSCC progression. Fourth, further mechanistic study is required to validate the pivotal role of FGF2 in mediating the function of miR-23a-3p in regulating the biological behavior of OSCC. Lastly, further downstream signaling of the miR-23a-3p-FGF2 axis should be investigated to comprehensively illustrate the biological function of miR-23a-3p in the development of OSCC.

In conclusion, our study reported for the first time, the biological function of miR-23a-3p in OSCC progression and identified FGF2 as its direct target. miR-23a-3p has exhibited the potential to be applied as a prognostic biomarker and an effective treatment target for OSCC. More clinical studies as well as animal experiments are essential to warrant its future clinical application.

Conflicts of interests

The authors declare that they have no conflicts of interests.

Acknowledgements

The authors thank the patients and volunteers participating in the research.

References

[1] J. Ferlay, I. Soerjomataram, R. Dikshit, et al., Cancer incidence and mortality

worldwide: sources, methods and major patterns in GLOBOCAN 2012, Int. J. Cancer (2014).
[2] Y. Sun, Y. Zhang, L. Liu, X. Song, G. Li, Genetic polymorphisms and HPV infection in oral squamous cell carcinomas, Curr. Opin. Virol. 14 (2015) 1–6.
[3] B.H. Wu, X.P. Xiong, J. Jia, W.F. Zhang, MicroRNAs: new actors in the oral cancer scene, Oral Oncol. 47 (5) (2011) 314–319.
[4] V. Ambros, The functions of animal microRNAs, Nature 431 (7006) (2004) 350–355.
[5] S. Volinia, G.A. Calin, C.G. Liu, et al., A microRNA expression signature of human solid tumors defines cancer gene targets, Proc. Natl. Acad. Sci. U. S. A. 103 (7) (2006) 2257–2261.
[6] Z. Liu, C. Diep, T. Mao, et al., MicroRNA-92b promotes tumor growth and activation of NF-κB signaling via regulation of NLK in oral squamous cell carcinoma, Oncol. Rep. 34 (6) (2015) 2961–2968.
[7] C. Liu, Z. Wang, Y. Wang, W. Gu, MiR-338 suppresses the growth and metastasis of OSCC cells by targeting NRP1, Mol. Cell. Biochem. 398 (1-2) (2015) 115–122.
[8] W.C. Huang, S.H. Chan, T.H. Jang, et al., miRNA-491-5p and GIT1 serve as modulators and biomarkers for oral squamous cell carcinoma invasion and metastasis, Cancer Res. 74 (3) (2014) 751–764.
[9] Y.C. Wen, W.J. Lee, P. Tan, et al., By inhibiting snail signaling and miR-23a-3p, osthole suppresses the EMT-mediated metastatic ability in prostate cancer, Oncotarget 6 (25) (2015) 21120–21136.
[10] Y. Li, H. Chen, P. She, et al., microRNA-23a promotes cell growth and metastasis in gastric cancer via targeting SPRY2-mediated ERK signaling, Oncol. Lett. 15 (6) (2018) 8433–8441.
[11] X. Hu, D. Chen, Y. Cui, Z. Li, J. Huang, Targeting microRNA-23a to inhibit glioma cell invasion via HOXD10, Sci. Rep. 3 (2013) 3423.
[12] S. Nayak, M.M. Goel, A. Makker, et al., Fibroblast growth factor (FGF-2) and its receptors FGFR-2 and FGFR-3 may Be putative biomarkers of malignant transformation of potentially malignant oral lesions into oral squamous cell carcinoma, PLoS One 10 (10) (2015) e0138801.
[13] I. Delrieu, The high molecular weight isoforms of basic fibroblast growth factor (FGF-2): an insight into an intracrine mechanism, FEBS Lett. 468 (1) (2000) 6–10.
[14] K. Harada, Kawashima Y. Supriatno, H. Yoshida, M. Sato, S-1 inhibits tumorigenicity and angiogenesis of human oral squamous cell carcinoma cells by suppressing expression of phosphorylated Akt, vascular endothelial growth factor and fibroblast growth factor-2, Int. J. Oncol. 30 (2) (2007) 365–374.
[15] C. Li, S. Shintani, N. Terakado, et al., Microvessel density and expression of vascular endothelial growth factor, basic fibroblast growth factor, and platelet-derived endothelial growth factor in oral squamous cell carcinomas, Int. J. Oral Maxillofac. Surg. 34 (5) (2005) 559–565.
[16] C. Wakulich, L. Jackson-Boeters, T.D. Daley, G.P. Wysocki, Immunohistochemical localization of growth factors fibroblast growth factor-1 and fibroblast growth factor-2 and receptors fibroblast growth factor receptor-2 and fibroblast growth factor receptor-3 in normal oral epithelium, epithelial dysplasias, and squamous cell carcinoma, Oral Surg. Oral Med. Oral Pathol. Oral Radiol. Endod. 93 (5) (2002) 573–579.
[17] X. Yang, H. Wu, T. Ling, Suppressive effect of microRNA-126 on oral squamous cell carcinoma in vitro, Mol. Med. Rep. 10 (1) (2014) 125–130.
[18] B. Zhou, R. Ma, W. Si, et al., MicroRNA-503 targets FGF2 and VEGFA and inhibits tumor angiogenesis and growth, Cancer Lett. 333 (2) (2013) 159–169.
[19] Q. He, X. Ren, J. Chen, et al., miR-16 targets fibroblast growth factor 2 to inhibit NPC cell proliferation and invasion via PI3K/AKT and MAPK signaling pathways, Oncotarget. 7 (3) (2016) 3047–3058.
[20] W. Guo, H. Wang, Y. Yang, et al., Down-regulated miR-23a contributes to the metastasis of cutaneous melanoma by promoting autophagy, Theranostics 7 (8) (2017) 2231–2249.
[21] F. Ma, W. Li, C. Liu, et al., MiR-23a promotes TGF-β1-induced EMT and tumor metastasis in breast cancer cells by directly targeting CDH1 and activating Wnt/β-catenin signaling, Oncotarget 8 (41) (2017) 69538–69550.
[22] L. Cheng, T. Yang, Y. Kuang, et al., MicroRNA-23a promotes neuroblastoma cell metastasis by targeting CDH1, Oncol. Lett. 7 (3) (2014) 839–845.
[23] H. Diao, Z. Ye, R. Qin, miR-23a acts as an oncogene in pancreatic carcinoma by targeting FOXP2, J. Investig. Med. 66 (3) (2018) 676–683.
[24] J. An, Y. Pan, Z. Yan, W. Li, J. Cui, J. Yuan, L. Tian, R. Xing, Y. Lu, MiR-23a in amplified 19p13.13 loci targets metallothionein 2A and promotes growth in gastric cancer cells, J. Cell. Biochem. 114 (9) (2013) 2160–2169.
[25] G. Wu, Z. Li, P. Jiang, et al., MicroRNA-23a promotes pancreatic cancer metastasis by targeting epithelial splicing regulator protein 1, Oncotarget 8 (47) (2017) 82854–82871.
[26] C. Siegel, J. Li, F. Liu, et al., miR-23a regulation of X-linked inhibitor of apoptosis (XIAP) contributes to sex differences in theresponse to cerebral ischemia, Proc. Natl. Acad. Sci. U. S. A. 108 (2011) 11662–11667.
[27] S. Jahid, J. Sun, R.A. Edwards, et al., miR-23a promotes the transition from indolent to invasive colorectal cancer, Cancer Discov. 2 (6) (2012) 540–553.
[28] Y. He, C. Meng, Z. Shao, et al., MiR-23a functions as a tumor suppressor in osteosarcoma, Cell. Physiol. Biochem. 34 (5) (2014) 1485–1496.